6. P. B. Robertson, M. R. Dence, M. A. Vos, in *Shock Metamorphism of Natural Materials*, B. M. French and N. M. Short, Eds. (Mono Book, Baltimore, 1968), pp. 433–452.
7. P. B. Robertson and R. A. F. Grieve, in *Impact and Explosion Cratering*, D. J. Roddy, R. O. Pepin, R. B. Merrill, Eds. (Pergamon, New York, 1977), pp. 687–702.
8. M. R. Dence, *NASA Publ. SP-380* (1977), p. 175; J. W. Head, in *Impact and Explosion Cratering*, D. J. Roddy, R. O. Pepin, R. B. Merrill, Eds. (Pergamon, New York, 1977), pp. 563–573.
9. W. C. Phinney and C. H. Simonds [in *Impact and Explosion Cratering*, D. J. Roddy, R. O. Pepin, R. B. Merrill, Eds. (Pergamon, New York, 1977), pp. 771–790] give diameter to depth ratios from 8 to 20 for the transient cavities of large terrestrial impact structures.
10. The probable impact origin of the Acraman structure was recognized during the course of mineral exploration in 1979–80. I thank the Broken Hill Proprietary Co. Ltd. for permission to use information contained in this paper. H. J. Melosh, E. M. Shoemaker, A. Hildebrand, and V. A. Gostin provided helpful comments on earlier drafts of this manuscript and D. J. Gilbert and P. W. Haines assisted with photomicrography.

2 December 1985; accepted 8 April 1986

Interleukin-2 Induction of T-Cell G_1 Progression and c-*myb* Expression

JULIE B. STERN AND KENDALL A. SMITH

In studies to determine the biochemical mechanisms responsible for cell proliferation, synchronized T cells were used as a model for cellular growth control. By metabolic and morphologic criteria, it was found that activation of the T-cell antigen receptor rendered the cells responsive to interleukin-2 (IL-2), but did not move them through the cell cycle. Instead, IL-2 stimulated G_1 progression to S phase, or lymphocyte "blastic transformation." During IL-2–promoted G_1 progression, expression of the cellular proto-oncogene c-*myb* was induced transiently at six to seven times basal levels, maximal levels occurring at the midpoint of G_1.

DESPITE THE DISCOVERY THAT MITOGENIC lectins induce T-cell proliferation (*1*), experimental approaches to the biochemical mechanisms responsible for promotion of T-cell cycle progression were fruitless until the elucidation of the crucial role of interleukin-2 (IL-2) [reviewed in (*2*)]. It is now recognized that T-cell DNA replication and mitosis, although dependent on activation of the T-cell antigen-receptor complex (*3*), is actually determined by a critical threshold of signals generated by the interaction of IL-2 with its specific membrane receptors (*4*). Even so, whether activation of the T-cell antigen-receptor complex promotes movement of the cells through G_1 to a point that requires IL-2 just before S phase, or whether IL-2 itself is responsible for G_1 progression, has remained unclear. Moreover, the intracellular molecular pathways triggered by IL-2 have thus far remained obscure.

To identify the metabolic and morphologic changes that occur during cell cycle progression, we synchronized human peripheral T cells into the G_0 phase of the cell cycle according to the following protocol (*4, 5*). Freshly isolated peripheral mononuclear cells are stimulated to express IL-2 receptors transiently by activation with monoclonal antibodies reactive with T3 (anti-T3), and then to undergo an asynchronous proliferative clonal expansion by supplementation with immunoaffinity-purified IL-2. After 14 days of culture, when IL-2 receptors are no longer expressed and the cells have reaccumulated in G_0, more than 99% of the cells are once again small resting T cells, and most (≥90%) express the T8 surface glycoprotein (*4–7*). Maximum IL-2 receptor expression can again be effected within 12 hours, in the absence of detectable IL-2 production, by stimulation with phorbol butyrate (*6, 7*), thereby permitting the dissociation of the effects of antigen receptor activation from those resulting from IL-2 receptor stimulation. This synchronized T-cell–IL-2 model system (*4*) is obligatory for the experimental dissection of the events that occur during T-cell cycle progression, because the effects of antigen receptor activation cannot be separated from IL-2 receptor triggering if primary, freshly isolated mononuclear cells are used. In the presence of accessory cells, polyclonal activating agents (mitogenic lectins, phorbol esters, and anti-T3) lead to both IL-2 production and IL-2 receptor expression by primary T cells within a few hours (*3, 5*). In contrast, phorbol esters stimulate only IL-2 receptor expression by T cells synchronized at 14 days, provided accessory cells are absent (*6, 7*).

When synchronized T cells are used, it is evident that activation of the T-cell antigen-receptor complex does not of itself move the cell population through G_1, which is generally defined as a gradual increase in cell size and cytoplasmic RNA content, culminating in DNA synthesis (*8*). Rather, IL-2 promotes both metabolic and morphologic changes in the cell population that are indicative of G_1 progression (Fig. 1). Cellular RNA content, monitored by tritiated uridine incorporation, increases only when IL-2 is added (Fig. 1A). Moreover, S-phase transition, which is dependent on IL-2, becomes detectable via tritiated thymidine incorporation only after 10 to 12 hours of IL-2 exposure, is maximal at 24 hours, and declines progressively over the next 24 to 48 hours (Fig. 1A). These metabolic changes are consistent with the IL-2–induced morphologic changes characteristic of G_1 progression (Fig. 1B). The cells remain small with dense nuclear chromatin after activation of the T-cell antigen-receptor complex, and only begin to undergo "blastic transformation" 5 to 10 hours after IL-2 exposure. Therefore, in terminology adopted from the extensively studied 3T3 cell cycle (*9, 10*), T cells become "competent" upon triggering of the T-cell antigen-receptor complex, whereas interaction of IL-2 with its receptor promotes T-cell cycle "progression."

T-cell competence induced by mitogenic lectins and phorbol esters is known to be associated with the expression of the cellular proto-oncogene c-*myc* (*11, 12*). In an effort to identify the expression of proto-oncogenes associated specifically with IL-2–induced metabolic and morphologic progression through G_1, we tested several additional oncogenes with the synchronized T cell–IL-2 model system. Expression of the cellular homolog of the oncogene of avian myeloblastosis virus (c-*myb*), which codes for a nuclear binding protein of unknown function (*13*), was noteworthy in the earliest experiments. As shown in Fig. 2, c-*myb* messenger RNA (mRNA) was undetectable in G_0 cells, whereas cells activated with phorbol butyrate and then exposed to IL-2 contained a single 3.8-kb species, the anticipated size of human c-*myb* mRNA (*14, 15*).

A detailed time course of c-*myb* expression after phorbol butyrate–induced competence and during IL-2–promoted G_1 progression revealed that c-*myb* was expressed solely during G_1 progression (Fig. 3). As shown in Fig. 3A, expression of c-*myb* remained at basal, undetectable levels throughout a 12-hour exposure to phorbol butyrate, whereas expression of c-*myc* increased tenfold during this interval. In contrast, c-*myb* expression first becomes detectable only during IL-2–

Department of Medicine, Dartmouth Medical School, Hanover, NH 03756.

induced G_1 progression, with maximal levels (sixfold induction) observed after 5 hours of IL-2 exposure, a time interval that precedes any detectable changes in cellular RNA content and morphology (compare Fig. 3B with Fig. 1). During this interval, c-*myc* mRNA levels were augmented only slightly over the tenfold increase mediated by phorbol butyrate, whereas readily detectable levels of c-*fos* and HLA-B7 mRNA transcripts remained constant at all of the time points tested, both after phorbol butyrate and during IL-2 stimulation.

To exclude the possibility that c-*myb* expression was somehow restricted to cells exposed to phorbol esters, we examined freshly isolated peripheral mononuclear cells after activation by anti-T3. As described earlier (*5*), and illustrated in Fig. 4A, proliferation beyond 3 days of culture is dependent upon IL-2 supplied exogeneously; removal of anti-T3 and IL-2 resulted in the cessation of proliferation by day 5. Thereafter, the cell population could be stimulated to reenter the cell cycle simply by the addition of IL-2, inasmuch as near maximal levels of IL-2 receptors were still expressed (*5–7*). Accordingly, a detailed time course of cell cycle progression (Fig. 4B) and c-*myb* expression (Fig. 4C) was analyzed upon reexposure of day 5 resting cells to immunoaffinity-purified IL-2. Cell cycle progression resumed within 12 hours; maximal levels of c-*myb* expression (sevenfold induction) preceded the onset of DNA synthesis by 6 hours in a fashion indistinguishable from that observed in cell populations activated secondarily by phorbol butyrate. Moreover, cells cultured in parallel in the absence of IL-2 did not express detectable levels of c-*myb* and did not undergo cell cycle progression.

The separation of the T-cell cycle into competence and progression stages is important because of the molecular implications of these functional terms. As monitored by the studies described in this report, the metabolic and morphologic consequences of T-cell cycle competence are minor in comparison with the changes that occur after IL-2–induced G_1 progression. Consequently, it is likely that the change from the IL-2–unresponsive stage to the competent stage (G_0 to G_1 transition) is associated with the expression of only a few select genes (notably the IL-2 receptor gene) (*4–7*), whereas IL-2–induced G_1 progression to S phase is mediated by the sequential activation of many genes. In this regard, in view of our previous observations (*4*), it is especially pertinent that maximum amounts of c-*myb* mRNA are observed after 5 hours of exposure to IL-2, just prior to detectable changes in morphology and in-

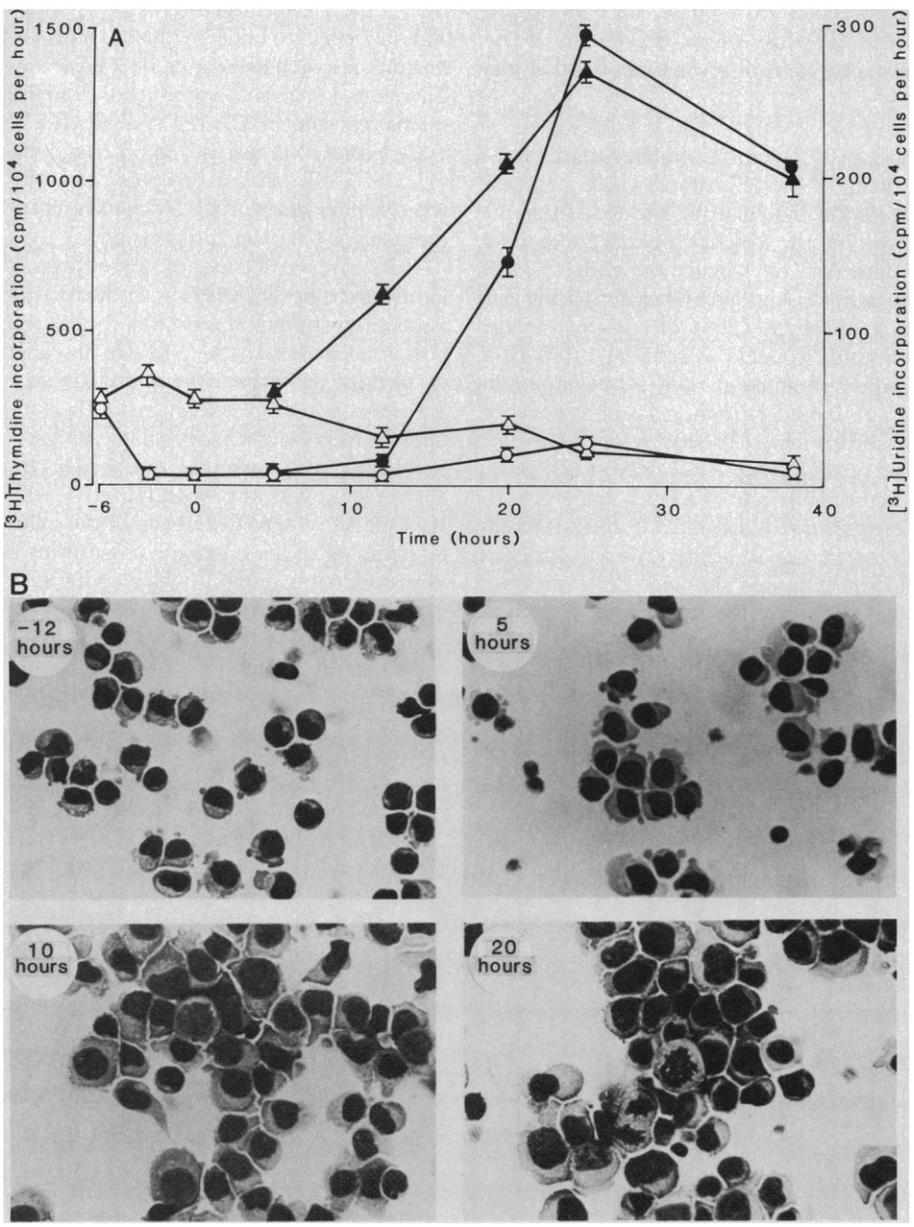

Fig. 1. Metabolic and morphologic analysis of T-cell cycle progression. (A) [^{3}H]Uridine incorporation (▲, △) and [^{3}H]thymidine incorporation (●, ○) by G_0-synchronized human T cells exposed for 6 hours to phorbol butyrate, then cultured from time 0 with immunoaffinity-purified IL-2 (*25*) (solid symbols) and IL-2–free medium (open symbols). Data shown are the means ± SEM of quadruplicate determinations corresponding to one of three separate experiments. (B) Wright-Giemsa–stained cytospin preparations of cells from an experiment performed as described in (A). G_0-synchronized cells before phorbol butyrate exposure (−12 hours); 5, 10, and 20 hours denote time of IL-2 exposure. Cells cultured for the same intervals without IL-2 showed no detectable change from those prior to phorbol butyrate stimulation (−12 hours). Human peripheral mononuclear cells isolated by Ficoll-Hypaque discontinuous gradient centrifugation were cultured (1×10^6 cells per milliliter) for 72 hours with anti-T3 (1:10,000 dilution, Ortho Diagnostics) in RPMI 1640 medium (Gibco) supplemented with 10% heat-inactivated (56°C for 45 minutes) fetal bovine serum (Sterile Systems), L-glutamine (300 μg/ml), penicillin G (50 U/ml), and gentamicin (50 μg/ml). The cells were then washed and maintained for 9 days at concentrations between 1×10^5 and 1×10^6 per milliliter by supplementation with immunoaffinity-purified IL-2 (500 p*M*) every 2 to 3 days. After 12 days, the cells were washed and cultured without IL-2 for 48 hours to ensure their reaccumulation in the G_0 phase of the cell cycle. IL-2 receptor reexpression was achieved by exposure to phorbol butyrate (50 ng/ml, Consolidated Midlands) for 6 to 12 hours, after which the cells were transferred to medium with IL-2 (500 p*M*) or to IL-2–free medium. Incorporation of [^{3}H]thymidine (2.0 μCi/ml, Schwarz/Mann Division, Becton Dickinson) and [^{3}H]uridine (2.0 μCi/ml) (New England Nuclear) incorporation was monitored at 2- to 4-hour intervals by liquid scintillation counting (*5*).

creased levels of [^{3}H]uridine incorporation. T-cell cycle progression depends on the duration of IL-2–receptor interaction, and exposure to IL-2 for 5 hours is essential for an irreversible progression to DNA replication (*4*). Inasmuch as the kinetics of appearance of cytoplasmic c-*myb* mRNA coincide with the time interval required for productive IL-2–receptor interactions, the data are consonant with the interpretation that a critical concentration of the c-*myb* gene product accumulates just before DNA replication.

The discovery that c-*myb* is expressed transiently during G_1 in synchronized mature peripheral T cells indicates that c-*myb* expression is not confined to immature hematopoietic cells, as suggested earlier (*14, 16, 17*). Instead, it is more likely that c-*myb* is expressed at high levels in hematopoietic tissues primarily because these tissues have a large fraction of cells undergoing proliferation. Moreover, the previous absence of detectable c-*myb* expression in other tissues could well reflect the limited number of cells in the proper cell cycle stage. Cell populations that are proliferating asynchronously may contain an insufficient proportion of cells undergoing G_1 progression to enable the detection of transient c-*myb* gene expression.

It may be particularly relevant that several cellular proto-oncogenes that code for nuclear binding proteins are expressed during normal cell cycle competence and progression. For example, both c-*fos* and c-*myc* are expressed transiently by 3T3 murine embryonic fibroblasts in response to the competence signals induced by platelet-derived growth factor and phorbol esters, but are not induced further during serum-stimulated G_1 progression (*11, 18–21*). Similarly, c-*myc* is expressed after activation of the T-cell antigen-receptor complex via mitogenic lectins (*11*) and phorbol esters (*12*), even in the presence of cycloheximide (*12, 22*), thereby excluding the possibility that IL-2 initiates c-*myc* expression. In addition, as described by others (*22, 23*) and illustrated by our data, IL-2 may also influence c-*myc* expression. It is perplexing that we did not detect any change in the expression of c-*fos*, in view of the findings with 3T3 cells (*19–21*). However, as c-*fos* expression is very transient after stimulation of 3T3 cells, it is possible that additional experiments will uncover a rapid appearance and disappearance of c-*fos* mRNA.

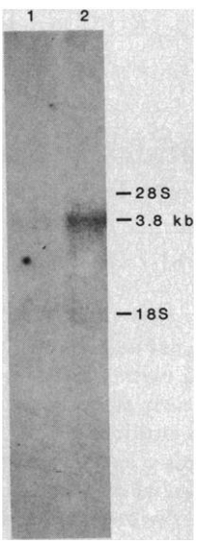

Fig. 2. Northern blot analysis of RNA from G_0-synchronized cells and from cells after IL-2–induced G_1 progression. RNA extracted from G_0-synchronized cells (lane 1) and IL-2–receptor–bearing cells exposed to IL-2 for 14 hours (lane 2) was hybridized with the radiolabeled 2.0-kb Eco RI genomic fragment of human c-*myb* (*25*). Total RNA was extracted from 1×10^8 cells by solubilization in 2.5 ml of 6.0*M* guanidine hydrochloride and 20 m*M* sodium acetate (*p*H 5.0). Liberated DNA was sheared by homogenization, and the cell extract was layered over a 1.5-ml cushion of 5.7*M* cesium chloride and 25 m*M* sodium acetate (*p*H 5.0). RNA was pelleted by centrifugation in a Beckman SW60 rotor at 34,000 rev/min for 20 hours at 20°C, then resuspended in H_2O and stored as an ethanol precipitate. RNA (10 μg) in 10 m*M* sodium phosphate (*p*H 7.0) was denatured for 1 hour at 50°C in 6.7% glyoxal and fractionated by electrophoresis on 1.5% agarose gels in 10 m*M* sodium phosphate containing ethidium bromide (500 ng/ml). After ribosomal bands were visualized under ultraviolet light, RNA was transferred onto nitrocellulose filters in 20× standard saline citrate (SSC), the filters were baked at reduced pressure for 2 hours at 80°C, and were pre-hybridized overnight at 42°C with 6× SSC [1× SSC: 0.15*M* sodium chloride and 15 m*M* sodium citrate (*p*H 7.0)] containing 1% sodium dodecyl sulfate (SDS), polyadenosine (50 μg/ml), sheared salmon sperm DNA (100 μg/ml) and 1× Denhardt's solution. Hybridization was performed at 40°C for 24 hours in 50% deionized formamide, 6× SSC, 0.1% SDS with 100 ng of ^{32}P-labeled probe (1×10^8 to 2×10^8 cpm per microgram of DNA). After high stringency washes with 0.1× SSC and 0.1% SDS (30 minutes at 20°C; 30 minutes at 60°C), radioactivity bound to the filters was detected by autoradiography.

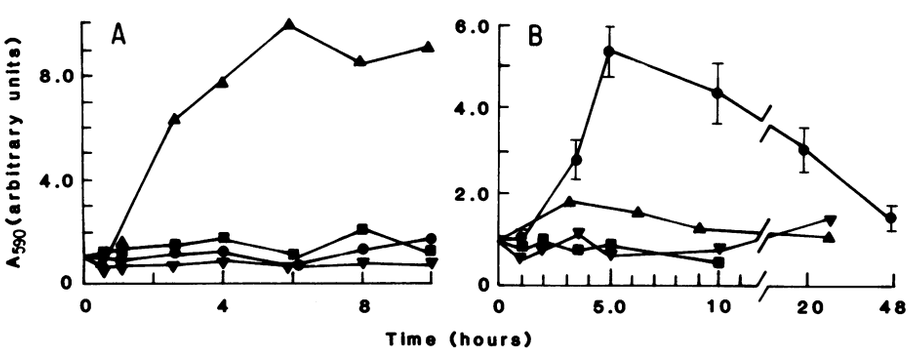

Fig. 3. Kinetics of c-*myb* expression during T-cell cycle progression. Total cellular RNA was extracted from G_0-synchronized cells, as described in the legend to Fig. 2, at various time intervals during (A) 10 hours of culture with phorbol butyrate, and (B) during 48 hours of IL-2 treatment after removal of phorbol butyrate. Equal amounts of total RNA (9, 3, and 1 μg) were applied to nitrocellulose filters (Schleicher & Schuell) with a dot-blot apparatus (Bethesda Research Laboratories) and were hybridized with radiolabeled probes to a 2.0-kb Eco RI genomic fragment of human c-*myb* (●) (*26*), 1.4-kb human HLA-B7 cDNA (▼) (*27*), 1.4-kb Cla I–Eco RI genomic fragment of human c-*myc* (▲) (*28*), and 1.5-kb Sst I–Eco RI + 5.3-kb Eco RI genomic fragments of mouse c-*fos* (■) (*29*).

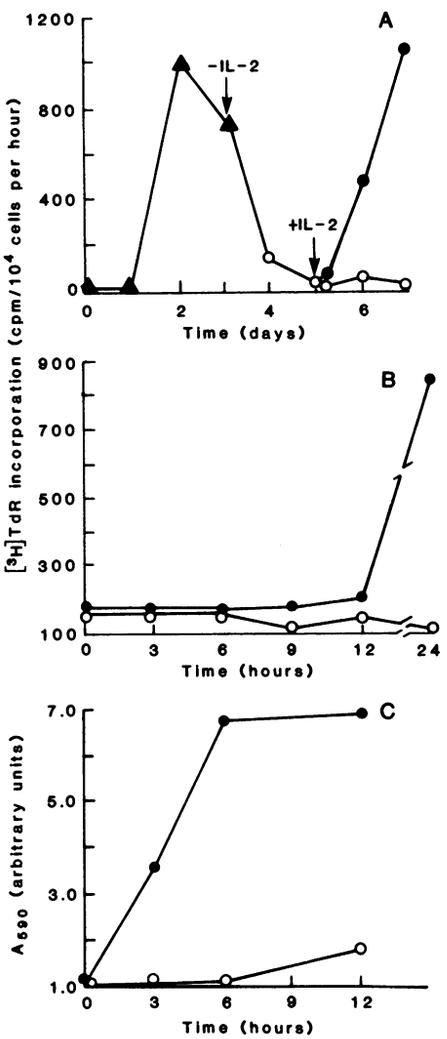

Fig. 4. IL-2–dependent cell cycle progression and c-*myb* expression by freshly isolated, primary T cells. (A) Kinetics of [^{3}H]thymidine incorporation in response to anti-T3 (▲), after removal of IL-2 (○), and after addition of IL-2 (500 p*M*) (●). (B) Detailed kinetics of [^{3}H]thymidine incorporation by day 5 cells exposed to IL-2 (500 p*M*) (●) or left unstimulated (○) in a separate experiment performed as in (A). (C) Scanning densitometric quantitation of dot-blot of total RNA from the cells described in (B) hybridized with a radiolabeled probe to human c-*myb*.

The collective data from studies performed with T cells and 3T3 cells indicate that cell cycle commitment is associated with expression of c-*fos* and c-*myc* proto-oncogenes, whereas c-*myb* expression is confined to G_1 progression. Thus, future experiments will surely focus on the critical functional consequences of nuclear binding by the products of the c-*fos*, c-*myc*, and c-*myb* genes during both normal and neoplastic cell proliferation.

Note added in proof. Subsequent to the submission of this manuscript for publication, a report by Thompson *et al.* (*24*) appeared, which confirms our findings and extends them to another species and other cell types; c-*myb* is expressed maximally during the midpoint of G_1 progression by chicken embryo fibroblasts, synchronized leukemic T cells, and bursal cells. An additional cell cycle–independent mechanism appears to result in an even more marked expression of c-*myb* in thymocytes.

REFERENCES AND NOTES

1. P. C. Nowell, *Cancer Res.* **20**, 462 (1960).
2. K. A. Smith, *Annu. Rev. Immunol.* **2**, 319 (1984).
3. S. C. Meuer *et al.*, *Proc. Natl. Acad. Sci. U.S.A.* **81**, 1509 (1984).
4. D. A. Cantrell and K. A. Smith, *Science* **224**, 1312 (1984).
5. ———, *J. Exp. Med.* **158**, 1895 (1983).
6. K. A. Smith, and D. A. Cantrell, *Proc. Natl. Acad. Sci. U.S.A.* **82**, 864 (1985).
7. M. Gullberg and K. A. Smith, *J. Exp. Med.* **163**, 270 (1986).
8. A. B. Pardee, B.-Z. Shilo, A. L. Koch, *Hormones and Cell Culture*, G. H. Sato and R. Ross, Eds. (Cold Spring Harbor Laboratory, Cold Spring Harbor, NY, 1979), vol. 6, pp. 373–392.
9. W. J. Pledger, C. D. Stiles, H. N. Antoniades, C. D. Scher, *Proc. Natl. Acad. Sci. U.S.A.* **74**, 4481 (1977).
10. ———, *ibid.* **75**, 2839 (1978).
11. K. Kelly, B. H. Cochran, C. D. Stiles, P. Leder, *Cell* **35**, 603 (1983).
12. M. Kronke, W. J. Leonard, J. M. Depper, W. C. Greene, *J. Exp. Med.* **161**, 1593 (1985).
13. K.-H. Klempnauer, G. Symonds, G. I. Evan, J. M. Bishop, *Cell* **37**, 537 (1984).
14. E. H. Westin *et al.*, *Proc. Natl. Acad. Sci. U.S.A.* **79**, 2194 (1982).
15. J. D. Mountz, A. D. Steinberg, D. M. Klinman, H. R. Smith, J. F. Mushinski, *Science* **226**, 1087 (1984).
16. J. H. Chen, *J. Virol.* **36**, 162 (1980).
17. T. J. Gonda, D. K. Sheiness, J. M. Bishop, *Mol. Cell. Biol.* **2**, 617 (1982).
18. J. Campisi, H. E. Gray, A. B. Pardee, M. Dean, G. F. Sonenshein, *Cell* **36**, 241 (1984).
19. M. E. Greenberg and E. B. Ziff, *Nature (London)* **311**, 433 (1984).
20. W. Kruijer, J. A. Cooper, T. Hunter, I. M. Verma, *ibid.* **312**, 711 (1984).
21. R. Muller, R. Bravo, J. Burckhardt, T. Curran, *ibid.*, p. 716.
22. J. C. Reed, D. E. Sabath, R. G. Hoover, M. B. Prystowsky, *Mol. Cell. Biol.* **5**, 3361 (1985).
23. J. C. Reed, P. C. Nowell, R. G. Hoover, *Proc. Natl. Acad. Sci. U.S.A.* **82**, 4221 (1985).
24. C. B. Thompson, P. B. Challoner, P. E. Neiman, M. Groudine, *Nature (London)* **319**, 374 (1986).
25. K. A. Smith, M. F. Favata, S. Oroszlan, *J. Immunol.* **131**, 1808 (1983).
26. G. Franchini, F. Wong-Staal, M. A. Baluda, C. Lengel, S. Tronick, *Proc. Natl. Acad. Sci. U.S.A.* **80**, 7385 (1983).
27. A. K. Sood, D. Pereira, S. M. Weissman, *ibid.* **78**, 616 (1981).
28. D. K. Watson, M. C. Psallidopoulos, K. P. Samuel, R. Dalla-Favera, T. S. Papas, *ibid.* **80**, 3642 (1983).
29. A. D. Miller, T. Curran, I. M. Verma, *Cell* **36**, 51 (1984).

30. Supported in part by grants from the National Cancer Institute (CA-17643), the American Tobacco Research Council, the Eli Lilly Corporation, and National Cancer Institute training grant CA-09367 (to J.S.).

6 December 1985; accepted 6 May 1986

Conformations of Signal Peptides Induced by Lipids Suggest Initial Steps in Protein Export

MARTHA S. BRIGGS,* DONALD G. CORNELL, RICHARD A. DLUHY, LILA M. GIERASCH†

Despite the requirement for a functional signal sequence in protein export, little is known of the conformational properties and membrane interactions of these highly hydrophobic amino terminal extensions on nearly all exported proteins. The *Escherichia coli* λ phage receptor signal sequence was studied in phospholipid monolayers by circular dichroism and Fourier transform infrared spectroscopy; the signal peptide was shown to prefer an α-helical conformation when inserted into the lipid phase. However, interaction with the lipid surface without insertion induced the signal sequence, which is unstructured in bulk aqueous solution, to adopt a β structure. These observations are combined in a model for the initial steps in signal sequence-membrane interaction in vivo.

THE NEARLY UNIVERSAL REQUIREMENT in protein export for an amino terminal extension, termed a "signal peptide," has focused attention on the roles that these highly hydrophobic sequences might play (*1*). While many essential details of the secretion process are still poorly understood, it is clear that the involvement of the signal sequence in both prokaryotic and eukaryotic protein secretion includes recognition by proteins, interactions with membranes or membrane-resident components, facilitation of translocation, and specific cleavability (*2, 3*). Little is known, however, of the physical characteristics that must influence their participation in the export process, such as conformational preferences or potentials for membrane and protein interaction.

Our biophysical studies on a family of chemically synthesized signal sequences from an *Escherichia coli* outer membrane protein, the λ phage receptor protein (LamB protein) (*4*), show that two physical properties of the isolated signal sequences, their tendency to adopt an α-helical conformation in hydrophobic environments and their tendency to insert into phospholipid monolayers, correlate with their in vivo export function (*5–7*). These properties may be involved in the same step in the secretion process or in different steps. An α-helical conformation may be required to generate a sufficiently hydrophobic structure to allow membrane insertion. Alternatively, the α helix may be necessary for binding to a protein, while the ability to interact with lipids may be important for translocation. To analyze further the relationships between these properties of signal sequences, we have designed experiments that enable conformational characterization of signal peptides in lipid monolayers.

Monolayers containing 65% 1-palmitoyl-2-oleoyl phosphatidylethanolamine (PE) and 35% 1-palmitoyl-2-oleoyl phosphatidylglycerol (PG) (a ratio chosen to mimic the *E. coli* membrane) and the wild-type LamB signal peptide were prepared for spectroscopic examination by transferring them to a solid support (Fig. 1). A miniature Teflon Langmuir/Wilhelmy trough with a dipping well was constructed to minimize the volume of subphase required. The lipid monolayers were formed by spreading of aliquots from chloroform solution until the desired initial pressure was achieved. Peptide was then immediately injected into the subphase. The film pressure was monitored for an equilibration period, after which the monolayer was transferred either to quartz plates [for circular dichroism (CD)] or to Ge crystals [for Fourier transform–infrared (FT-IR)]. Monolayer transfer and spectroscopic investigations fol-

M. S. Briggs and L. M. Gierasch, Department of Chemistry, University of Delaware, Newark, DE 19716.
D. G. Cornell, Eastern Regional Research Center, U.S. Department of Agriculture, 600 East Mermaid Lane, Philadelphia, PA 19118.
R. A. Dluhy, National Center for Biomedical Infrared Spectroscopy, Battelle-Columbus Laboratories, 505 King Avenue, Columbus, OH 43201.

*Present address: Department of Chemistry, University of Pennsylvania, Philadelphia, PA 19104.
†To whom correspondence should be addressed.